Liver Research 8 (2024) 259–268

Contents lists available at ScienceDirect

Liver Research

journal homepage: http://www.keaipublishing.com/en/journals/liver-research

Original Article

Growth differentiation factor 7 alleviates the proliferation and metastasis of hepatocellular carcinoma

Jianyong Zhuo [a, 1], Huigang Li [b, 1], Peiru Zhang [c, 1], Chiyu He [b], Wei Shen [b], Xinyu Yang [b], Zuyuan Lin [b], Runzhou Zhuang [d], Xuyong Wei [e, f], Shusen Zheng [f, g, h], Xiao Xu [e, f, i, **], Di Lu [e, f, *]

[a] *Department of Hepatobiliary and Pancreatic Surgery, Affiliated Hangzhou First People's Hospital, School of Medicine, Westlake University, Hangzhou, Zhejiang, China*
[b] *Zhejiang University School of Medicine, Hangzhou, Zhejiang, China*
[c] *The Fourth School of Clinical Medicine, Zhejiang Chinese Medical University, Hangzhou, Zhejiang, China*
[d] *Department of Thoracic Surgery, The First Affiliated Hospital, Zhejiang University School of Medicine, Hangzhou, Zhejiang, China*
[e] *Department of Hepatobiliary & Pancreatic Surgery and Minimally Invasive Surgery, Zhejiang Provincial People's Hospital (Affiliated People's Hospital), Hangzhou Medical College, Hangzhou, Zhejiang, China*
[f] *NHC Key Laboratory of Combined Multi-organ Transplantation, Hangzhou, Zhejiang, China*
[g] *Department of Hepatobiliary and Pancreatic Surgery, The First Affiliated Hospital, Zhejiang University School of Medicine, Hangzhou, Zhejiang, China*
[h] *Department of Hepatobiliary and Pancreatic Surgery, Shulan (Hangzhou) Hospital, Hangzhou, Zhejiang, China*
[i] *Institute of Translational Medicine, Zhejiang University, Hangzhou, Zhejiang, China*

ARTICLE INFO

Article history:
Received 23 January 2024
Received in revised form
11 June 2024
Accepted 28 September 2024

Keywords:
Hepatocellular carcinoma (HCC)
Growth differentiation factor 7 (GDF7)
JunB proto-oncogene (JUNB)
Epithelial–mesenchymal transition (EMT)
Proliferation
Metastasis

ABSTRACT

Background and aims: Inflammatory factors play significant roles in the development and occurrence of hepatocellular carcinoma (HCC). However, the tumor-protective functions of growth differentiation factors (GDFs) in HCC are yet to be clarified. In this study, we aimed to evaluate the expression levels of 10 GDFs in tumor and paratumor tissues from patients with HCC and perform *in vitro* and *in vivo* experiments to elucidate the role of GDF7 in regulating the proliferation and metastasis of HCC.
Methods: The gene expression of 10 GDFs was compared between HCC and paratumors using The Cancer Genome Atlas dataset and patient-derived tissues. A tumor microarray containing 108 HCC tissue samples was used to explore the prognostic value of GDF7 expression. Loss-of-function experiments were also performed *in vitro* and *in vivo* to investigate the role of GDF7 in HCC.
Results: The mRNA and protein levels of GDF7 were significantly lower in HCC tumors than in paratumors ($P < 0.001$). Kaplan–Meier analysis showed that decreased GDF7 expression in HCC was associated with worse overall survival (5-year rate: 61.8% *vs.* 27.5%, $P < 0.001$) and increased recurrence risk ($P < 0.001$). Multivariate Cox regression analysis demonstrated that low GDF7 expression, the presence of microvascular invasion, and elevated alpha-fetoprotein (AFP) levels were independent risk factors for tumor recurrence and poor survival. Downregulation of GDF7 also increased the tumor growth in HCC cells and in an HCC xenograft model. GDF7 knockdown promoted migration and invasion via epithelial–mesenchymal transition. Meanwhile, a negative correlation between JunB proto-oncogene (JUNB) and GDF7 was observed in HCC tissues. Modulating JUNB levels altered GDF7 protein expression.
Conclusions: GDF7 is a potential biomarker for predicting superior outcomes in patients with HCC. GDF7 amplification is a potential therapeutic option for HCC.

* Corresponding author. Department of Hepatobiliary & Pancreatic Surgery and Minimally Invasive Surgery, Zhejiang Provincial People's Hospital (Affiliated People's Hospital), Hangzhou Medical College, Hangzhou, Zhejiang, China.
** Corresponding author. Department of Hepatobiliary & Pancreatic Surgery and Minimally Invasive Surgery, Zhejiang Provincial People's Hospital (Affiliated People's Hospital), Hangzhou Medical College, Hangzhou, Zhejiang, China.
E-mail addresses: zjxu@zju.edu.cn (Xiao Xu), zjuludi@zju.edu.cn (Di Lu).
[1] These authors contributed equally to this work.

https://doi.org/10.1016/j.livres.2024.09.006

1. Introduction

Hepatocellular carcinoma (HCC) is the most common type of primary liver cancer and ranks as the third leading cause of cancer-related mortality worldwide.[1] The majority of HCCs occur in cases of chronic liver diseases characterized by hepatic inflammation, such as hepatitis B or C virus infection, alcohol abuse, and non-alcoholic fatty liver disease.[2] In the malignant environment, liver inflammatory cells release various soluble factors, including cytokines, chemokines, growth factors, prostaglandins, and proangiogenic factors, creating the tumor microenvironment that serves a dual function, having directly and indirectly promote or inhibit tumors.[3,4] However, the exact role of certain inflammatory factors in HCC has not been explored.

Growth differentiation factors (GDFs) belong to the transforming growth factor-beta (TGF-β) superfamily and play essential roles in cell differentiation, phenotype, and function.[5] To date, 10 GDFs have been reported, namely, GDF1, GDF2, GDF3, GDF5, GDF6, GDF7, GDF9, GDF10, GDF11, and GDF15.[6] Several GDFs have been shown to promote tumor survival. For example, Ratnam *et al.*[7] demonstrated that the depletion of pancreatic adenocarcinoma-derived GDF15 suppressed tumor development in Kras-induced tumor xenografts by inhibiting the cytotoxic activity of macrophages. In addition, Cheng *et al.*[8] reported that GDF1 overexpression in HCC significantly enhanced tumor metastatic abilities, despite the inhibitory effect on tumor proliferation. However, whether GDFs exert tumor-inhibiting functions has not yet been clarified.

Here, we analyzed the expression levels of these 10 GDFs in HCC tumor and paratumor tissues. GDF7, also known as bone morphogenic protein 12, is one of the most significantly downregulated molecules in HCC tumors. It has been suggested to be involved in tendon repair and regeneration, osteogenic differentiation, and immune regulation.[9–11] However, the role of GDF7 in tumors remains unclear. Therefore, we evaluated the expression of GDF7 in tumor and paratumor tissues from patients with HCC and performed *in vitro* and *in vivo* experiments to elucidate the role of GDF7 in regulating the proliferation and metastasis of HCC.

2. Methods

2.1. Ethical approval

This study was approved by the Ethics Committee of Shulan (Hangzhou) Hospital (No. KY2021014) and The First Affiliated Hospital, Zhejiang University School of Medicine (No. 2018-768), and was conducted following the tenets of the Declaration of Helsinki. All patients provided written informed consent before the study. All animal procedures were performed in accordance with the Guide for the Care and Use of Laboratory Animals from the USA National Institutes of Health (NIH), and the protocols were approved by the Animal Experiment Ethics Committee of Zhejiang University School of Medicine (No. ZJU2022-24131).

2.2. Specimen collection

Thirty paired primary tumor tissues and corresponding normal tissues were collected from patients with HCC who underwent liver transplantation at Shulan (Hangzhou) Hospital between October 2021 and March 2022. The tumor microarray cohort included 108 patients with HCC who underwent liver transplantation at The First Affiliated Hospital, Zhejiang University School of Medicine, between January 2015 and December 2017, as previously described.[12] The follow-up ended on December 31, 2021.

2.3. Immunohistochemistry (IHC)

Tumor tissue microarray sections were obtained in our previous study.[12] The slides were deparaffinized, dehydrated, and retrieved in citrate buffer. The next day, the slides were incubated with primary antibodies against GDF7 (#ab189928, Abcam, Cambridge, MA, USA), JunB proto-oncogene (JUNB, #3753T, Cell Signaling Technology, Danvers, MA, USA), E-cadherin (#3195T, Cell Signaling Technology, Danvers, MA, USA), N-cadherin (#13116T, Cell Signaling Technology, Danvers, MA, USA), Vimentin (#5741T, Cell Signaling Technology, Danvers, MA, USA), and Ki67 (#ab21700, Abcam, Cambridge, MA, USA). The slides were subjected to 3,3′-diaminobenzidine (DAB) staining prior to visualization.

IHC staining was scored by two independent pathologists blinded to the clinical characteristics of the patients. A semiquantitative scoring system (no staining = 0, weak staining = 1, moderate staining = 2, strong staining = 3) and percentages of positive cells (<5% = 0, 5%–25% = 1, 26%–50% = 2, 51%–75% = 3, >75% = 4) were used to estimate the results, as previously described.[13] The final immune reactivity score was calculated by multiplying the intensity score by the percentage score, ranging from 0 to 12. According to the final immune reactive score, the IHC result was classified as 0–6, negative (−) or 7–12, positive (+).

2.4. Cell culture

Human HCC cell lines, Hep3B and SK-Hep-1, were obtained from the Type Culture Collection of the Chinese Academy of Sciences (Shanghai, China). The cell lines were cultured in Dulbecco's modified Eagle's medium (DMEM) (Genom, Hangzhou, China) supplemented with 10% fetal bovine serum (FBS) (Gibco, Grand Island, NY, USA) and 1% penicillin/streptomycin (Solarbio, Beijing, China) in a 5% CO_2 incubator (Thermo Fisher Scientific, Waltham, MA, USA) at 37 °C.

2.5. Quantitative real-time polymerase chain reaction (qPCR)

Total RNA was extracted from HCC samples using an RNA-Quick Purification Kit (#RN001, YiShan Biotech, Shanghai, China) and used as a template to generate cDNA using a Reverse Transcription Kit (#RR233-01, Vazyme, Nanjing, China). qPCR was performed using QuantStudio5 (Thermo Fisher Scientific, Waltham, MA, USA). All primer sequences are listed in Supplemental Table 1.

2.6. Transfection

Small interfering RNA (siRNA), short hairpin RNA (shRNA), and lentiviral particles were constructed by Guannan Co., Ltd. (Hangzhou, China). JetPRIME (#101000046, Polyplus Transfection, Illkirch, France) was used for the transient transfection of siRNAs or shRNAs into cells, in accordance with the manufacturer's instructions. Lentiviral particles were produced and transfected into the cells to obtain stable clones. The sequences for the siRNAs targeting JUNB (siJUNB) were as follows: siJUNB#1, 5′-ACAAGGUGAAGACGCUCAA-3′, siJUNB#2, 5′-GCCUCUCUCUACACGACUA-3′, siJUNB#3, 5′-GCAUCAAAGUGGAGCGCAA-3′. The sequences for the shRNAs targeting GDF7 (shGDF7) were as follows: shGDF7#1, 5′-GCAGAGGAAAGAGAGCTTATT-3′, shGDF7#2, 5′-GAGAGCTTATTCCGGGAGATC-3′, shGDF7#3, 5′-CGCACGCAGAGGAAAGAGATT-3′.

2.7. Western blotting

Cells were lysed with radioimmunoprecipitation assay (RIPA) buffer containing proteinase inhibitors at the indicated time points. Cell lysates were quantified using a BCA Protein Assay Kit (#23225,

Thermo Fisher Scientific, Waltham, MA, USA). Protein lysates were electrophoresed and transferred to polyvinylidene fluoride (PVDF) membranes (Merck Millipore, Darmstadt, Germany). Then, the membranes were incubated with primary antibodies against β-actin (#81115-1-RR, Proteintech, Wuhan, China), GDF7 (#ab189928, Abcam, Cambridge, MA, USA), E-cadherin (#3195T, Cell Signaling Technology, Danvers, MA, USA), N-cadherin (#13116T, Cell Signaling Technology, Danvers, MA, USA), Vimentin (#5741T, Cell Signaling Technology, Danvers, MA, USA), Snail (#3879T, Cell Signaling Technology, Danvers, MA, USA), and JUNB (#3753T, Cell Signaling Technology, Danvers, MA, USA).

2.8. Cell viability and colony formation assay

Cultured cells were seeded in 96-well plates at a density of 10^3 cells/well. At the indicated time points, the cells were incubated with 10 μL/well of cell counting kit-8 (CCK-8) reagent (#HY-K0301, MedChem Express, Monmouth Junction, NJ, USA). After 2 h of incubation, optical density (OD) values were determined using a microplate reader (BioTek, Winooski, VT, USA) at a wavelength of 450 nm.

For the colony formation assay, cultured cells were seeded in six-well plates at a density of 10^3 cells and cultured for 14 days. Cell colonies were fixed and stained with 0.1% crystal violet. Colony numbers were counted using ImageJ software (the National Institutes of Health, USA).

2.9. Transwell assay

Cell migration and invasion assays were performed in 24-well plates with Transwell inserts (Corning Inc., Corning, NY, USA), with or without Matrigel (#356234, BD Biocoat, Corning, NY, USA). In each assay, 10^5 cultured cells were suspended in 200 μL of serum-free DMEM (Genom, Hangzhou, China) in the upper chamber of the wells and 1000 μL of DMEM (Genom, Hangzhou, China) with 10% FBS (Gibco, Grand Island, NY, USA) was placed in the lower chamber. The cells were incubated for 24–48 h, and the cells on the lower membrane surface were fixed and stained with 0.1% crystal violet. Cells were counted in five randomly selected fields under a microscope (Olympus, Tokyo, Japan).

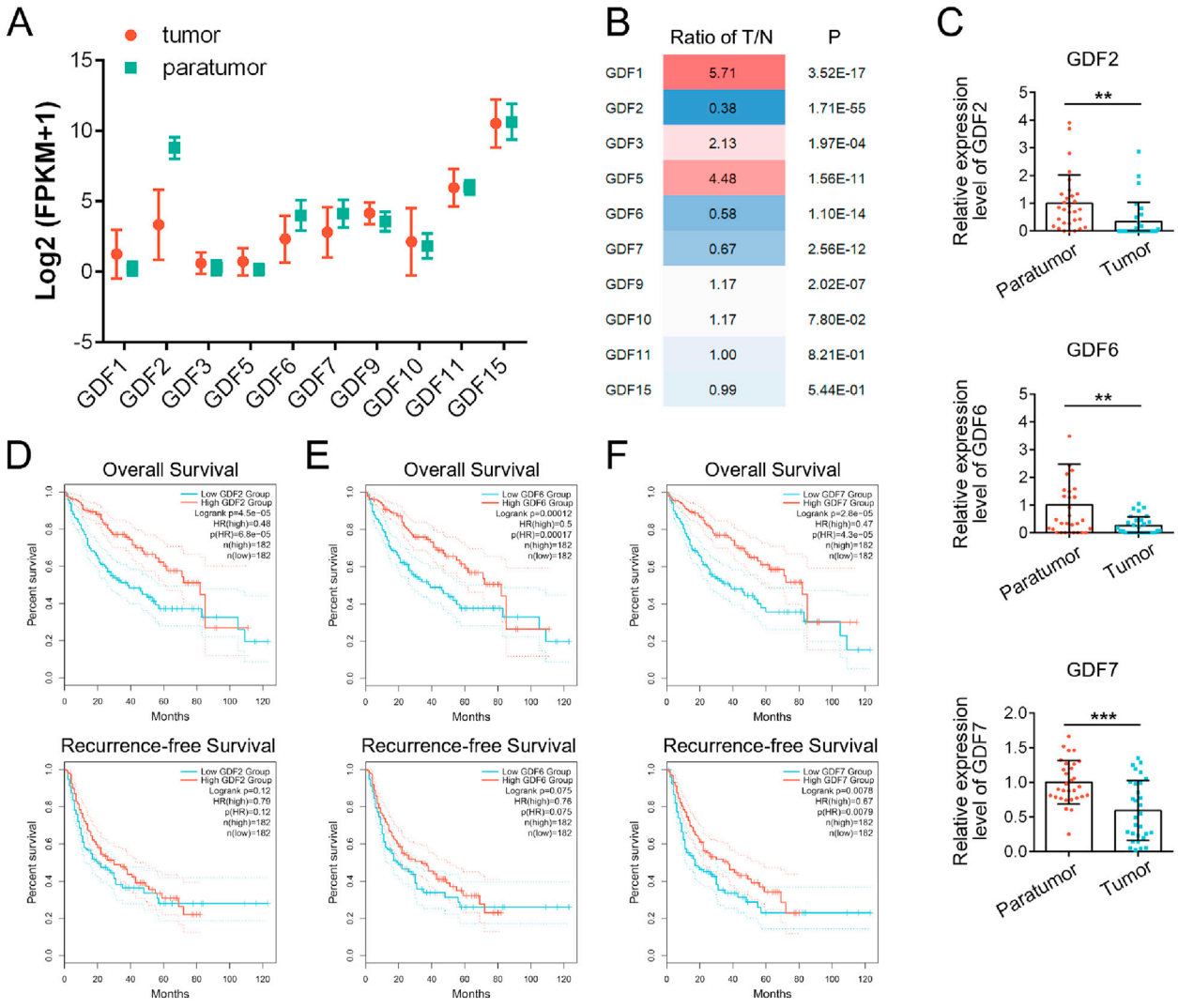

Fig. 1. Identifying the tumor-protective growth differentiation factor (GDF) genes. (A) The gene expression of 10 GDFs between hepatocellular carcinoma (HCC) and tumor-adjacent tissues in The Cancer Genome Atlas (TCGA) data and **(B)** comparison of differential expression of every GDF gene in HCC and tumor-adjacent tissues using TCGA data. The red block indicates increased expression in tumor, whereas the blue block indicates decreased expression in tumor. T, tumor; N, nontumor. **(C)** The mRNA expression levels of GDF2, GDF6, and GDF7 in the paired HCC and tumor-adjacent tissues ($n = 30$). Compared by paired Student's *t*-test. $^{**}P < 0.01$, $^{***}P < 0.001$. Kaplan–Meier analysis of the overall survival and recurrence-free survival in terms of differential expression groups based on **(D)** GDF2, **(E)** GDF6, and **(F)** GDF7. Analyzed by GEPIA (http://gepia.cancer-pku.cn/).

2.10. In vivo growth assay

Four-week-old, male, nude mice were purchased from GemPharmatech (Nanjing, China). All mice were acclimated to a 12-h light/dark cycle under specific pathogen-free conditions.

The cultured cells were resuspended at a density of 5×10^7 cells/mL in a 1:1 volumetric mixture of serum-free DMEM (Genom, Hangzhou, China) and Matrigel (BD Biocoat, Corning, NY, USA). The cells were then injected subcutaneously into the upper left flank of 4-week-old nude mice. The tumor size was estimated twice a week using a digital caliper. The tumor volume was calculated as follows: (maximum diameter) × (minimum diameter) × (minimum diameter)/2. When the tumor size exceeded 2000 mm^3 or the animal's weight dropped by >20%, the mice were sacrificed.

2.11. Luciferase reporter assays

The GDF7 promoter was constructed into a pGL3-reporter plasmid (Hangzhou Aoqian Biosystems Co. Ltd, Hangzhou, China) for the luciferase reporter assay. HCC cells overexpressing JUNB or control were transiently transfected with a GDF7 luciferase reporter using the jetPRIME transfection reagent (#101000046, Polyplus Transfection, Illkirch, France). Two days after transfection, the cells were collected and lysed and the extracts were assayed in technical triplicates for firefly and Renilla luciferase activity using the dual-luciferase reporter assay (#E1910, Promega, Madison, WI, USA), in accordance with the manufacturer's instructions.

2.12. Statistical analysis

Statistical analyses were performed using SPSS version 23 (IBM Corp, Armonk, NY, USA) and GraphPad Prism version 6 (La Jolla, CA, USA). Relationships with clinicopathological characteristics were analyzed using chi-squared test, and the Kaplan–Meier method, followed by the log-rank test, was used for survival analysis. Cox regression was used to estimate hazard ratios with 95% confidence intervals (CIs). The measured values were expressed as the mean ± standard deviation. Unless otherwise indicated, all statistical analyses in the experiments were performed using unpaired two-tailed Student's *t*-tests. Differences were considered significant at *P*-value <0.05.

3. Results

3.1. GDF7 is significantly downregulated in HCC

We used data from The Cancer Genome Atlas (TCGA) to screen for GDF genes that are abnormally expressed in HCC. Among this gene family, four genes, GDF1, GDF3, GDF5, and GDF9, were significantly upregulated in HCC tumors compared with the levels in paratumor tissues. Meanwhile, three genes, GDF2, GDF6, and GDF7, were significantly downregulated in HCC tissues (Fig. 1A and B). We further investigated 30 paired HCC and corresponding paratumor tissues to validate TCGA analysis. The qPCR results showed that the mRNA expression of GDF2, GDF6, and GDF7 in HCC was

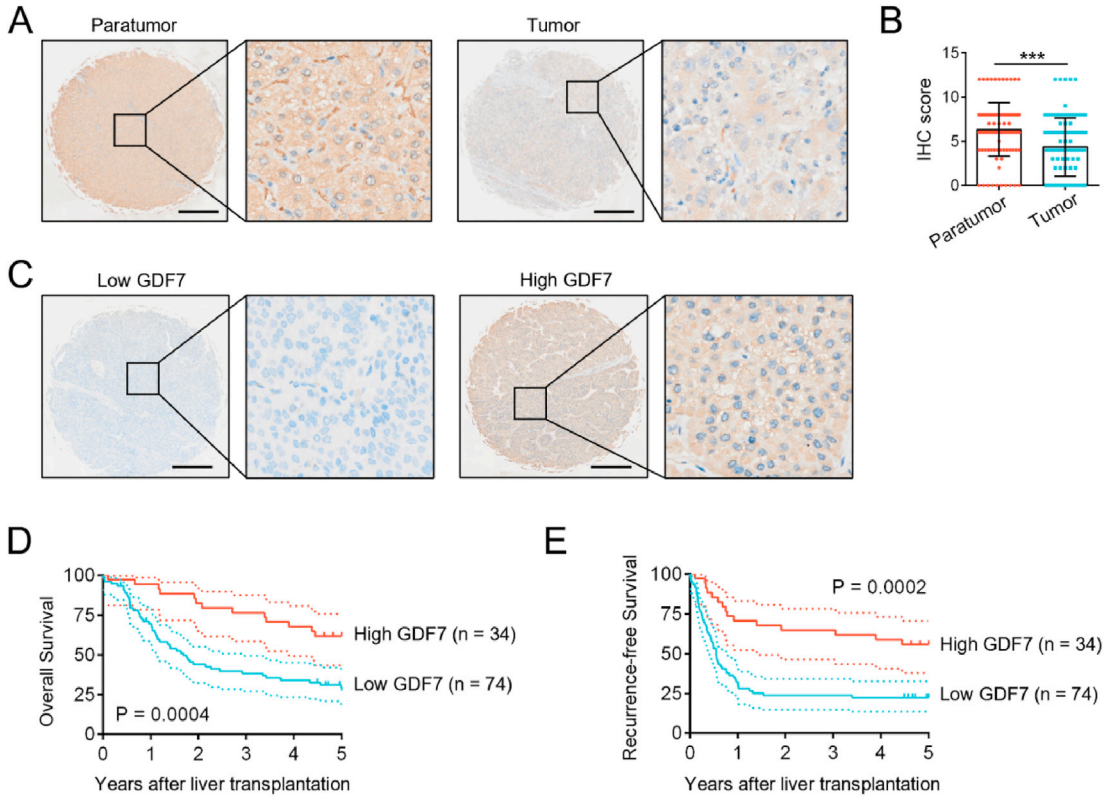

Fig. 2. Decreased expression of growth differentiation factor 7 (GDF7) is associated with worse outcomes in patients with hepatocellular carcinoma (HCC). (A) Representative images of GDF7 expression in HCC tissues and corresponding adjacent tissues, as detected by immunohistochemistry (IHC). Scale bars, 400 μm. **(B)** A scatter diagram of semiquantitative GDF7 score in HCC tissues and corresponding paratumor tissues ($n = 108$). Compared by paired Student's *t*-test. $^{***}P < 0.001$. **(C)** Representative images of low and high GDF7 expression in HCC tissues, as detected by IHC. Scale bars, 400 μm. Kaplan–Meier survival curves showing **(D)** overall survival and **(E)** recurrence-free survival in HCC with low ($n = 74$) and high GDF7 expression ($n = 34$). Compared by log-rank test.

significantly reduced, which matched the results of TCGA analysis (Fig. 1C). The overall survival (OS) and recurrence-free survival (RFS) of the three downregulated GDFs were further investigated using GEPIA (http://gepia.cancer-pku.cn/) (Fig. 1D–F). The findings showed that the differential expression of GDF7 significantly affected both OS and RFS (Fig. 1E). The other two downregulated genes GDF2 and GDF6 failed to influence RFS (Fig. 1D and F). These findings indicate that GDF7 may play a tumor-suppressive role in HCC.

3.2. Low GDF7 expression is associated with poor prognosis in patients with HCC

To explore the prognostic role of GDF7 expression in HCC, we enrolled 108 patients with HCC who underwent liver transplantation. Tumor microarray analysis showed that GDF7 protein expression in HCC tissues was significantly lower than that in the paired paratumor liver tissues, which was consistent with the results at the mRNA level (Fig. 2A and B). Based on GDF7 expression in HCC tissues, patients in the tumor microarray cohort were divided into low- ($n = 74$) and high-GDF7 groups ($n = 34$) (Fig. 2C). The demographic and clinicopathological features of these groups are shown in Table 1. Lower GDF7 expression in HCC is associated with more tumor nodules, hepatitis B infection, elevated alpha-fetoprotein (AFP) levels, and tumor recurrence.

Kaplan–Meier analysis showed that patients with low GDF7 expression had worse OS ($P = 0.0004$) and RFS ($P = 0.0002$) than those with high GDF7 expression (Fig. 2D and E). The 1-, 3-, and 5-year OS rates in the GDF7-high group were 94.1%, 76.5%, and 61.8%, whereas they were 69.5%, 38.3%, and 27.5% in the GDF7-low group, respectively. Moreover, the 1-, 3-, and 5-year RFS rates in the GDF7-high group were 70.6%, 64.7%, and 55.9%, whereas the corresponding values in the GDF7-low group were 32.2%, 23.8%, and 22.4%, respectively. Furthermore, multivariate Cox regression analysis demonstrated that the presence of microvascular invasion, elevated AFP levels, and low GDF7 levels were independent predictors of high risk of tumor recurrence and poor OS (Tables 2 and 3).

3.3. GDF7 knockdown promotes aggressive phenotypes in HCC

As the loss of GDF7 has been implicated in worse clinical outcomes in HCC, we assessed whether GDF7 disruption in tumor cells exacerbated the aggressive phenotypes. We detected the protein expression levels of GDF7 in HCC cell lines and immortalized normal liver cell line (LO2) and selected two cell lines with high GDF7 expression (Hep3B and SK-Hep-1) for subsequent experiments (Fig. 3A). We used shRNA to knock down GDF7 expression in these cell lines and confirmed the efficiency of GDF7 knockdown using Western blotting (Fig. 3B). Compared with the corresponding control cells, proliferation and colony formation were increased in cells with GDF7 knockdown (Fig. 3C and D). *In vivo* mouse xenograft experiments showed that Hep3B cells with GDF7 knockdown produced dramatically larger tumors than the corresponding control cells (Fig. 3E and F).

We further determined whether loss of function of GDF7 influences the capacity for tumor metastasis. The data showed that the rates of migration and invasion were increased in cells with GDF7 knockdown compared with those in the corresponding control cells

Table 1
General information and clinicopathological characteristics of patients with low- and high-GDF7 expression in hepatocellular carcinoma tissues.

Variables	Low-GDF7 group ($n = 74$)	High-GDF7 group ($n = 34$)	*P*-value
Age, *n* (%)			0.896
≤50 years	36 (48.6)	17 (50.0)	
>50 years	38 (51.4)	17 (50.0)	
Sex, *n* (%)			0.503
Male	70 (94.6)	31 (91.2)	
Female	4 (5.4)	3 (8.8)	
HBsAg presence, *n* (%)			0.006
Yes	71 (95.9)	27 (79.4)	
No	3 (4.1)	7 (20.6)	
Liver cirrhosis, *n* (%)			0.944
Yes	72 (97.3)	33 (97.1)	
No	2 (2.7)	1 (2.9)	
Presurgical TACE, *n* (%)			0.535
Yes	41 (55.4)	21 (61.8)	
No	33 (44.6)	13 (38.2)	
Child–Pugh score, *n* (%)			0.132
A/B	56 (75.7)	30 (88.2)	
C	18 (24.3)	4 (11.8)	
Serum AFP, *n* (%)			0.019
≤400 ng/mL	39 (52.7)	26 (76.5)	
>400 ng/mL	35 (47.3)	8 (23.5)	
Tumor number, *n* (%)			0.010
≤3	42 (56.8)	28 (82.4)	
>3	32 (43.2)	6 (17.6)	
Tumor size, *n* (%)			0.326
≤5 cm	36 (48.6)	20 (58.8)	
>5 cm	38 (51.4)	14 (41.2)	
Tumor differentiation, *n* (%)			0.184
Well/moderate	27 (36.5)	17 (50.0)	
Poor	47 (63.5)	17 (50.0)	
Microvascular invasion, *n* (%)			0.087
Yes	37 (50.0)	11 (32.4)	
No	37 (50.0)	23 (67.6)	
Tumor recurrence, *n* (%)			0.001
Yes	51 (68.9)	12 (35.3)	
No	23 (31.1)	22 (64.7)	

Abbreviations: AFP, alpha-fetoprotein; GDF7, growth differentiation factor 7; HBsAg, hepatitis B surface antigen; TACE, transarterial chemoembolization.

Table 2
Univariable and multivariable Cox regression analyses of the variables for overall survival (OS) in 108 patients with hepatocellular carcinoma.

Variables		Univariable predictors of OS		Multivariable predictors of OS	
		HR (95% CI)	*P*-value	HR (95% CI)	*P*-value
Age	≤50 years	1			
	>50 years	0.888 (0.546–1.444)	0.632		
Sex	Male	1			
	Female	0.708 (0.284–1.765)	0.458		
HBsAg presence	No	1			
	Yes	1.643 (0.597–4.525)	0.336		
Liver cirrhosis	No	1			
	Yes	2.675 (0.371–19.294)	0.329		
Presurgical TACE	No	1			
	Yes	0.992 (0.606–1.625)	0.974		
Child–Pugh score	A or B	1			
	C	2.555 (1.491–4.378)	0.001	1.732 (0.987–3.040)	0.056
Serum AFP	≤400 ng/mL	1			
	>400 ng/mL	2.422 (1.478–3.969)	<0.001	1.857 (1.118–3.082)	0.017
Tumor number	≤3	1			
	>3	2.589 (1.581–4.238)	<0.001	1.681 (0.998–2.831)	0.051
Tumor size	≤5 cm	1			
	>5 cm	1.483 (0.909–2.420)	0.114		
Tumor differentiation	Well or moderate	1			
	Poor	1.930 (1.145–3.253)	0.014	1.266 (0.709–2.263)	0.425
Microvascular invasion	No	1			
	Yes	2.822 (1.715–4.644)	<0.001	1.931 (1.127–3.309)	0.017
GDF7 expression	Low	1			
	High	0.342 (0.186–0.631)	0.001	0.471 (0.251–0.885)	0.019

Abbreviations: AFP, alpha-fetoprotein; CI, confidence interval; GDF7, growth differentiation factor 7; HBsAg, hepatitis B surface antigen; HR, hazard ratio; TACE, transarterial chemoembolization.

Table 3
Univariable and multivariable Cox regression analyses of the variables for recurrence-free survival (RFS) in 108 patients with hepatocellular carcinoma.

Variables		Univariable predictors of RFS		Multivariable predictors of RFS	
		HR (95% CI)	*P*-value	HR (95% CI)	*P*-value
Age	≤50 years	1			
	>50 years	0.677 (0.425–1.078)	1.000		
Sex	Male	1			
	Female	0.517 (0.223–1.195)	0.123		
HBsAg presence	No	1			
	Yes	2.065 (0.752–5.666)	0.159		
Liver cirrhosis	No	1			
	Yes	0.346 (0.107–1.121)	0.077	0.436 (0.130–1.462)	0.179
Presurgical TACE	No	1			
	Yes	0.988 (0.618–1.578)	0.959		
Child–Pugh score	A or B	1			
	C	2.209 (1.300–3.755)	0.003	1.440 (0.816–2.540)	0.208
Serum AFP	≤400 ng/mL				
	>400 ng/mL	2.600 (1.621–4.170)	<0.001	1.990 (1.224–3.236)	0.006
Tumor number	≤3	1			
	>3	2.744 (1.710–4.404)	<0.001	1.659 (0.998–2.758)	0.051
Tumor size	≤5 cm	1			
	>5 cm	1.732 (1.083–2.771)	0.022	1.329 (0.800–2.207)	0.272
Tumor differentiation	Well or moderate	1			
	Poor	1.765 (1.084–2.874)	0.022	1.224 (0.676–2.215)	0.505
Microvascular invasion	No	1			
	Yes	3.132 (1.943–5.050)	<0.001	2.307 (1.366–3.898)	0.002
GDF7 expression	Low	1			
	High	0.343 (0.193–0.608)	<0.001	0.425 (0.236–0.766)	0.004

Abbreviations: AFP, alpha-fetoprotein; CI, confidence interval; GDF7, growth differentiation factor 7; HBsAg, hepatitis B surface antigen; HR, hazard ratio; TACE, transarterial chemoembolization.

(Fig. 4A and B). As epithelial–mesenchymal transition (EMT) is a crucial event for cancer cell metastasis,[14] At both mRNA and protein levels, HCC cells with GDF7 knockdown had stronger expression of mesenchymal marker genes, N-cadherin, Vimentin, and Snail, but weaker expression of the epithelial marker gene E-cadherin than the corresponding control cells (Fig. 4C and D). Meanwhile, the immunohistochemistry results showed that compared with the control, tumor with GDF7 knockdown from tumor-bearing mice had higher

expression levels of N-cadherin, Vimentin, and Ki67 but lower expression levels of E-cadherin (Fig. 4E).

3.4. GDF7 is downregulated by JUNB overexpression

To clarify which transcription factor regulates the expression of GDF7, we used JASPAR analysis (https://jaspar.genereg.net/) and observed that JUNB is a potential transcription factor binding to the GDF7 promoter (Fig. 5A). Luciferase reporter assays showed that compared with the control group, the JUNB-overexpression group had lower luciferase activity, which indicated GDF7's promoter activity (Fig. 5B). Furthermore, the protein expression of GDF7 in Hep3B and SK-Hep-1 cells with JUNB overexpression decreased compared with that in the corresponding control cells (Fig. 5C). Conversely, the knockdown of JUNB with siRNA resulted in increased GDF7 expression compared with that in the control cells with untargeted siRNA (Fig. 5D). The correlation between GDF7 levels and JUNB expression in HCC tumors was evaluated in the tumor microarray cohort. JUNB expression was negatively associated with GDF7 expression ($P = 0.01$, Fig. 5E and F). These results indicated that GDF7 is a downstream target of JUNB.

4. Discussion

The malignant nature of HCC is thought to be associated with the particular characteristics of its tumor microenvironment. Cytokines and chemokines play important roles in the crosstalk between tumor and immune cells. GDF7, a cytokine belonging to the TGF-β superfamily, is involved in tendon repair and regeneration, osteogenesis differentiation, and immune regulation.[9–11] Unlike other GDFs, which are associated with poor outcomes in cancer, we focused on the protective role of GDF7 in HCC progression.

In this study, we observed that low GDF7 expression in tumor tissues was associated with a poor prognosis in patients with HCC. These findings indicate that GDF7 expression is negatively associated with HCC malignancy. We showed that GDF7 inhibited tumor growth *in vitro* and *in vivo* and suppressed the migration and invasion of HCC cells. Although our study demonstrated via GEPIA

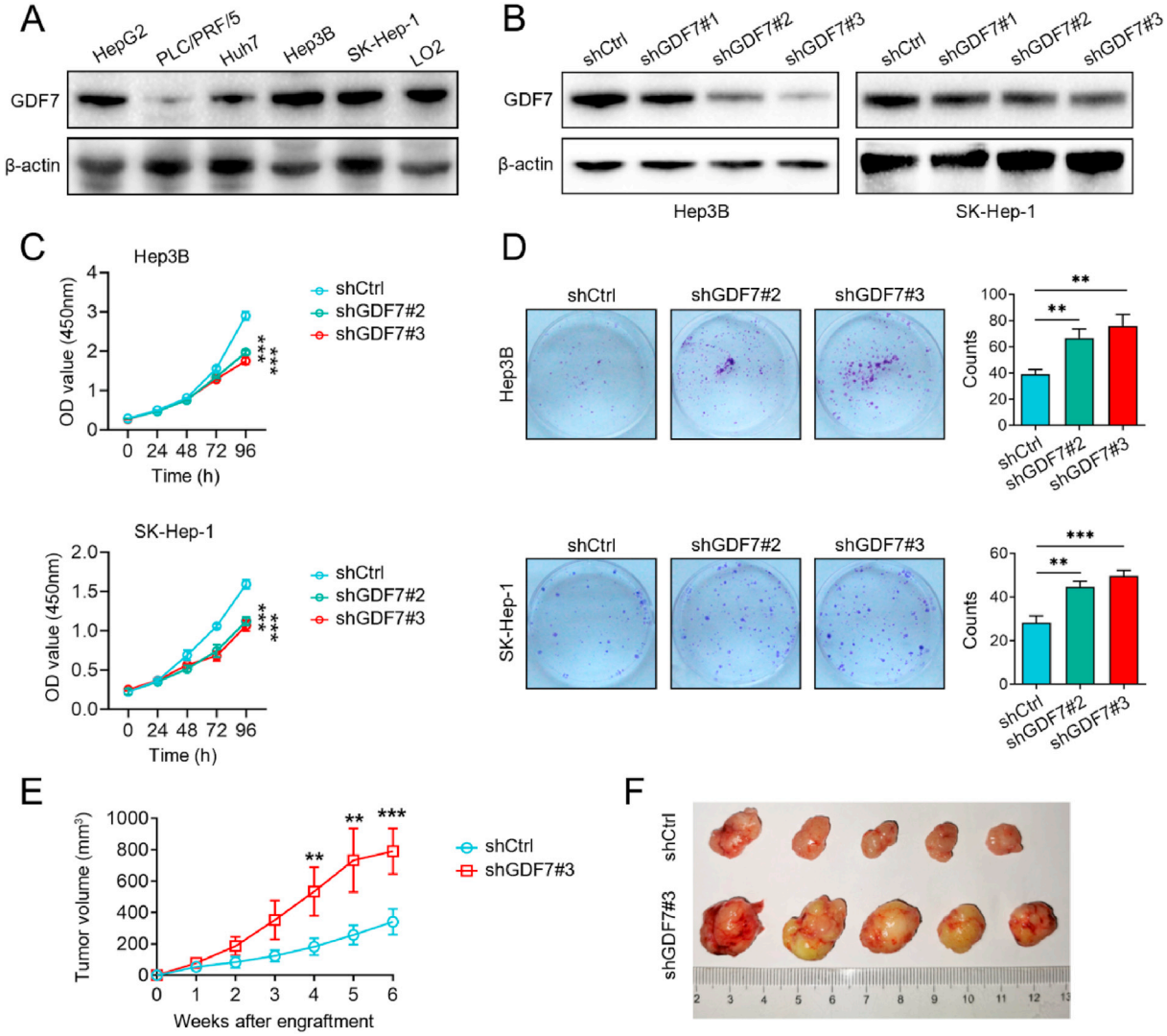

Fig. 3. GDF7 knockdown promotes HCC tumor proliferation and growth. (A) The protein expression of GDF7 in different cell lines, detected by Western blotting. **(B)** Immunoblot analysis of protein extracts from Hep3B and SK-Hep-1 cells treated with control (shCtrl) and three shRNA sequences of GDF7. **(C)** CCK-8 assay and **(D)** colony formation assay in Hep3B and SK-HEP-1 cells treated with shCtrl and shGDF7. **(E)** Tumor growth curves and **(F)** images of tumors from tumor-bearing mice ($n = 5$ per group). The data are shown as the mean ± standard deviation. Compared by Student's *t*-test. $^{**}P < 0.01$, $^{***}P < 0.001$. Abbreviations: CCK-8, cell counting kit-8; GDF7, growth differentiation factor 7; HCC, hepatocellular carcinoma; OD, optical density.

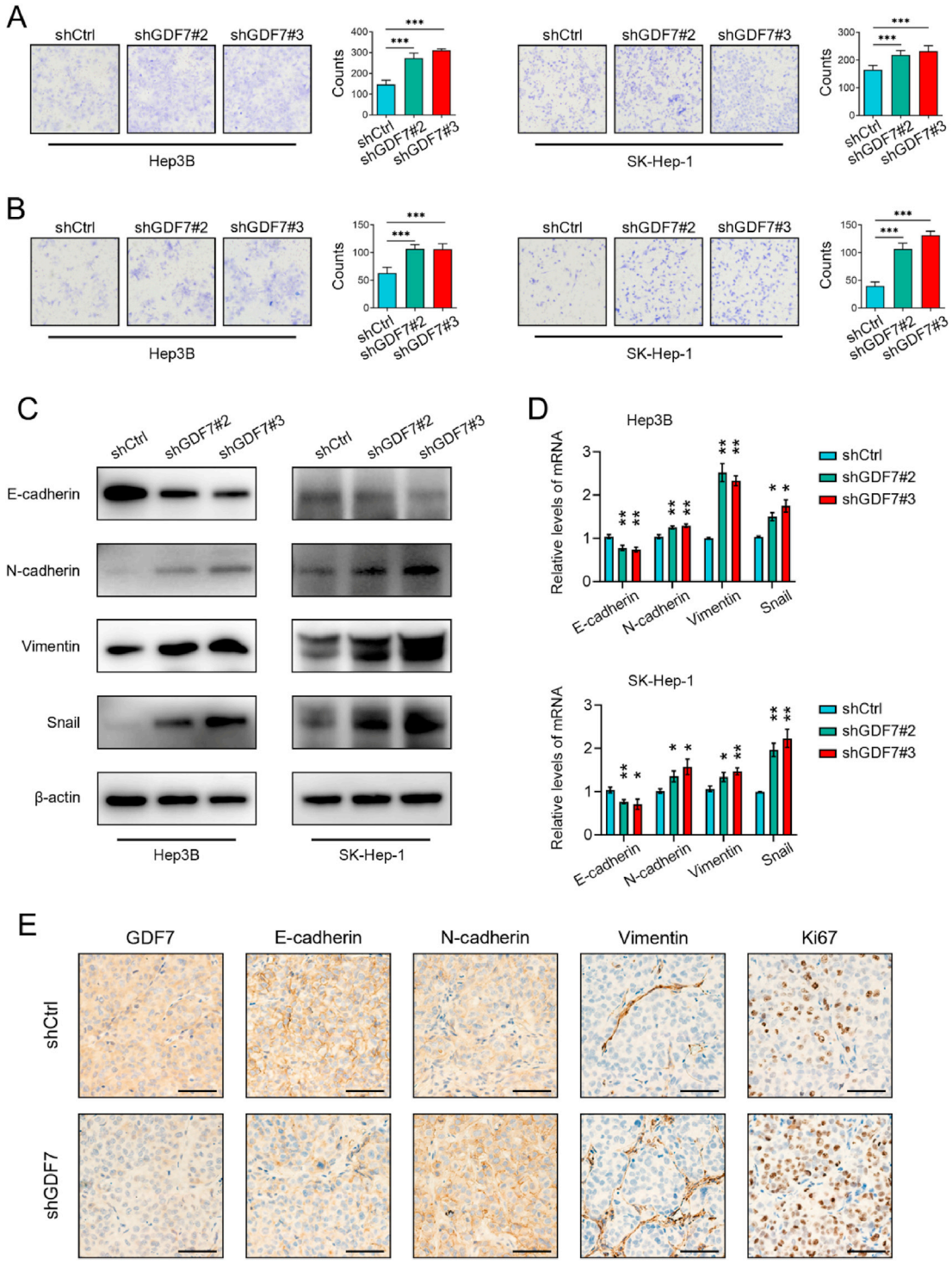

Fig. 4. Growth differentiation factor 7 (GDF7) knockdown increases migration and invasion in hepatocellular carcinoma (HCC) cells. Representative images and data of **(A)** migration and **(B)** invasion in Hep3B and SK-Hep-1 cells treated with shCtrl and shGDF7. **(C)** The expression of epithelial–mesenchymal transition (EMT)-related proteins in shCtrl and shGDF7 of Hep3B and SK-Hep-1 cells, detected by Western blotting. **(D)** The mRNA levels of EMT-related markers in Hep3B and SK-Hep-1 cells with GDF7 knockdown. **(E)** Representative images of EMT-related markers and Ki-67 in tumors from tumor-bearing mice, detected by immunohistochemistry. Scale bars, 40 μm. The data are shown as the mean ± standard deviation. Compared by Student's *t*-test. $^{*}P < 0.05$, $^{**}P < 0.01$, $^{***}P < 0.001$.

that the high expression of GDF2 or GDF6 was associated with superior survival, several studies have shown opposite functions in different cancer types. GDF6 is reported to maintain Ewing sarcoma growth by preventing Src hyperactivation and to promote melanoma progression by governing an embryonic cell gene signature.[15,16] Meanwhile, GDF2 promotes HCC angiogenesis by activating hypoxia inducible factor-1alpha (HIF-1α)/vascular endothelial growth factor A (VEGFA) expression, and targeting GDF2 has been shown to achieve notable therapeutic efficacy for HCC and colorectal cancer.[17,18] Chen *et al.*[19] reported that GDF2–inhibitor of DNA-binding protein 1 (ID1) signaling plays an essential role in promoting tumor stemness in EpCAM-positive

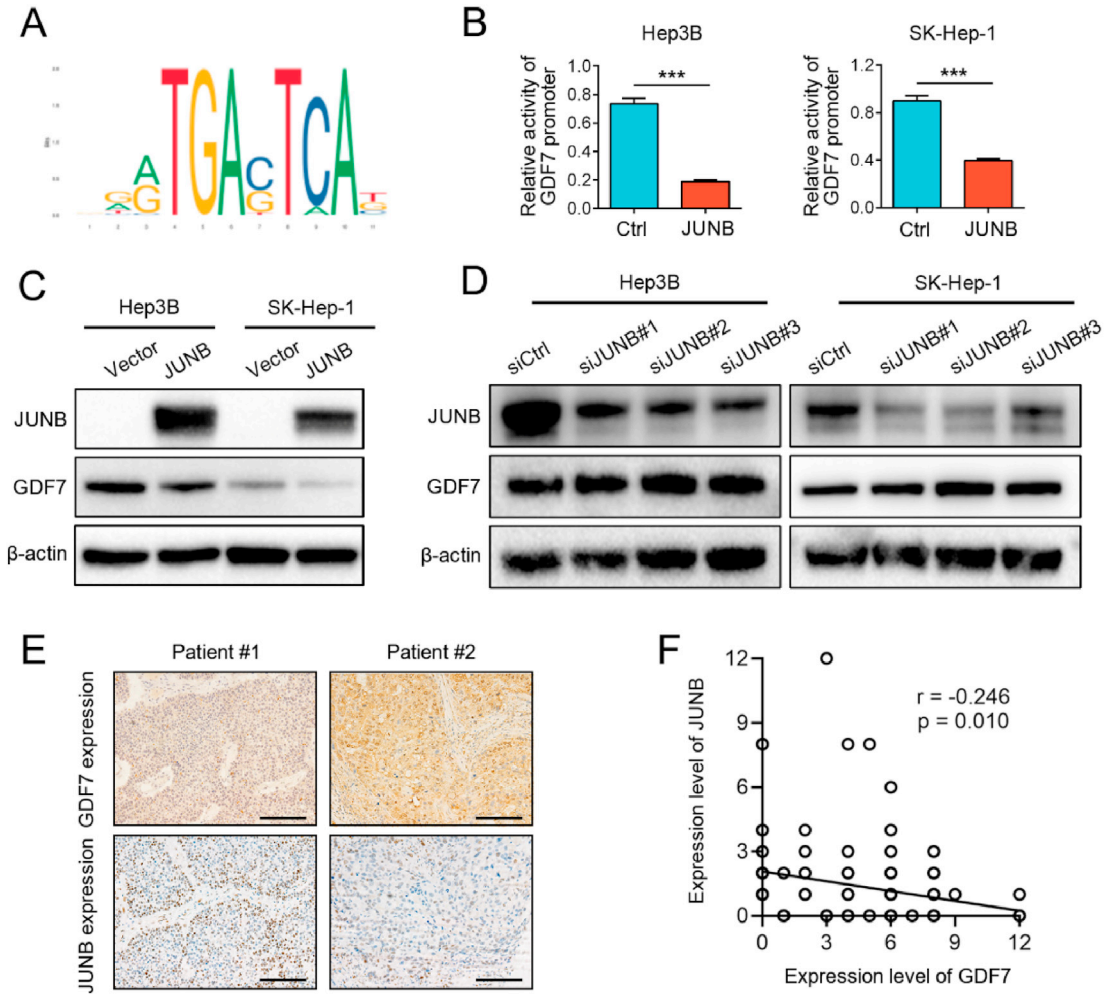

Fig. 5. GDF7 is downregulated by JUNB overexpression. (A) The potential binding site of JUNB to the GDF7 promoter, predicted by JASPAR analysis (https://jaspar.genereg.net/). **(B)** Detection of GDF7 promoter activity after the overexpression of JUNB in Hep3B and SK-Hep-1 cells by dual-luciferase reporter assay. The data are shown as mean ± standard deviation. Compared by Student's *t*-test. $^{***}P < 0.001$. **(C)** The GDF7 protein expression in Ctrl and JUNB overexpression of Hep3B and SK-Hep-1 cells, detected by Western blotting. **(D)** The GDF7 protein expression in Ctrl and JUNB-knockdown Hep3B and SK-Hep-1 cells, detected by Western blotting. **(E)** Representative images of GDF7 and JUNB expression in clinical HCC tissues. Scale bars, 100 μm. **(F)** The correlation between GDF7 levels and JUNB expression in HCC tumors was evaluated in the tumor microarray cohort ($n = 108$) using Pearson's correlation analysis. Abbreviations: GDF7, growth differentiation factor 7; HCC, hepatocellular carcinoma; JUNB, JunB proto-oncogene.

HCC. The roles of GDF2 and GDF6 in HCC are controversial, and further investigation is needed. The above background shows that the role of GDF7 in HCC is unique and differs from those of other growth differentiation factors.

Limited research has been performed on the mechanism that regulates GDF7 expression. Only two studies have suggested that GDF7 expression is regulated by RNA methylation. Song *et al.*[20] reported that the GDF7 promoter region exhibited remarkable m6A methylation in endometrial cancer. Moreover, Wan *et al.*[21] showed that an activated ten-eleven translocation enzyme could hypomethylate the GDF7 promoter region, leading to GDF7 protein overexpression. Our results demonstrated that JUNB acts as a negative regulator of the transcription of GDF7. JUNB is a critical component of the activator protein-1 transcription factor and acts either as a tumor suppressor or as an oncogene, depending on the cellular context.[22–24] Recently, Pérez-Benavente *et al.*[25] used tumor genomic data to demonstrate that JUNB amplification is associated with poor prognosis in breast and ovarian cancers. They further reported that JUNB could enhance tumor growth and metastasis in a mouse model by switching the response of TGF-β2 stimulation from an antiproliferative to a proinvasive one.[25] Noguchi *et al.*[26] used luciferase-based reporter assays to indicate that JUNB overexpression increased bone morphogenetic protein 6 transcription. Therefore, we concluded that JUNB is a key regulator mediating GDF7 expression in HCC.

EMT is crucial for cancer cell metastasis.[14] The results of the *in vitro* experiment indicated that GDF7 could inhibit the migration and invasion of HCC tumor cells. Several studies have also shown that GDF family members (GDF8, 9, and 11) regulate the expression of the EMT marker Snail via the SMAD pathway.[27–29] The SMAD pathway may mediate GDF7-induced downregulation of the expression of EMT markers. Increasing evidence has suggested that the GDF superfamily is involved in immune regulation. Ratnam *et al.*[7] identified that the nuclear factor-kappaB (NF-κB)/GDF15 regulatory axis is important for the metastasis of pancreatic adenocarcinoma via the evasion of macrophage immune surveillance.[7] Meanwhile, endogenously high expression of GDF15 was found to contribute to the proliferation and immune escape of malignant gliomas.[30] Cheng *et al.*[8] also showed that GDF1 enhanced the expression of cancer-testis antigens, which stimulated the immunogenicity of HCC cells via the ALK7/SMAD2/3 signaling cascade.[8] The above studies suggested that GDF7 plays an important role in tumor immunity, which warrants further investigation.

A limitation of this study is that we did not clarify whether and how exogenous supplementation of GDF7 inhibit the growth and metastasis of tumor cell. Further investigations are needed.

5. Conclusions

In conclusion, GDF7 is a potential biomarker for predicting superior outcomes in patients with HCC. Disruption of GDF7 expression could exacerbate the progression of HCC, and GDF7 activation is a potential cancer-directed therapeutic option.

Authors' contributions

Jianyong Zhuo, Huigang Li, and Peiru Zhang contributed equally to this work. **Jianyong Zhuo:** Writing – original draft, Methodology, Conceptualization. **Huigang Li:** Visualization, Validation, Software, Methodology. **Peiru Zhang:** Software, Methodology. **Chiyu He:** Visualization, Methodology. **Wei Shen:** Visualization, Software. **Xinyu Yang:** Software, Formal analysis. **Zuyuan Lin:** Visualization, Methodology. **Runzhou Zhuang:** Resources. **Xuyong Wei:** Formal analysis, Data curation. **Shusen Zheng:** Resources, Data curation. **Xiao Xu:** Writing – review & editing, Supervision, Funding acquisition. **Di Lu:** Writing – review & editing, Project administration, Conceptualization.

Data availability statement

All the datasets are available from the corresponding authors on reasonable request.

Declaration of competing interest

The authors declare that there is no conflicts of interest.

Acknowledgements

This work was granted by the National Key Research and Development Program of China (No. 2021YFA1100500), the Major Research Plan of the National Natural Science Foundation of China (No. 92159202), the Key Research & Development Plan of Zhejiang Province (No. 2021C03118), the National Natural Science Foundation of China (No. 82303387 and No. 82300742), the Natural Science Foundation of Zhejiang Province (No. LQ23H160048 and No. LQ22H160052), and the Health Science & Technology Plan of Zhejiang Province (No. 2022RC060). It was also supported by the Construction Fund of Medical Key Disciplines of Hangzhou (No. OO20200093).

Appendix A. Supplementary data

Supplementary data to this article can be found online at https://doi.org/10.1016/j.livres.2024.09.006.

References

1. Llovet JM, Kelley RK, Villanueva A, et al. Hepatocellular carcinoma. *Nat Rev Dis Primers*. 2021;7:6. https://doi.org/10.1038/s41572-020-00240-3.
2. Mak LY, Cruz-Ramón V, Chinchilla-López P, et al. Global epidemiology, prevention, and management of hepatocellular carcinoma. *Am Soc Clin Oncol Educ Book*. 2018;38:262–279. https://doi.org/10.1200/EDBK_200939.
3. Pocino K, Stefanile A, Basile V, et al. Cytokines and hepatocellular carcinoma: biomarkers of a deadly embrace. *J Pers Med*. 2022;13:5. https://doi.org/10.3390/jpm13010005.
4. Ait-Ahmed Y, Lafdil F. Novel insights into the impact of liver inflammatory responses on primary liver cancer development. *Liver Res*. 2023;7:26–34. https://doi.org/10.1016/j.livres.2023.01.001.
5. Guignabert C, Humbert M. Targeting transforming growth factor-βreceptors in pulmonary hypertension. *Eur Respir J*. 2021;57:2002341. https://doi.org/10.1183/13993003.02341-2020.
6. Katoh Y, Katoh M. Comparative integromics on BMP/GDF family. *Int J Mol Med*. 2006;17:951–955.
7. Ratnam NM, Peterson JM, Talbert EE, et al. NF-κB regulates GDF-15 to suppress macrophage surveillance during early tumor development. *J Clin Invest*. 2017;127:3796–3809. https://doi.org/10.1172/JCI91561.
8. Cheng W, Li HL, Xi SY, et al. Growth differentiation factor 1-induced tumour plasticity provides a therapeutic window for immunotherapy in hepatocellular carcinoma. *Nat Commun*. 2021;12:7142. https://doi.org/10.1038/s41467-021-27525-9.
9. Wang D, Zhang X, Ng KW, et al. Growth and differentiation factor-7 immobilized, mechanically strong quadrol-hexamethylene diisocyanate-methacrylic anhydride polyurethane polymer for tendon repair and regeneration. *Acta Biomater*. 2022;154:108–122. https://doi.org/10.1016/j.actbio.2022.10.029.
10. Zhou Y, Liu S, Wang W, et al. The miR-204-5p/FOXC1/GDF7 axis regulates the osteogenic differentiation of human adipose-derived stem cells via the AKT and p38 signalling pathways. *Stem Cell Res Ther*. 2021;12:64. https://doi.org/10.1186/s13287-020-02117-4.
11. Xu W, Tang HJ, Anwaier A, et al. Immunogenomic characteristics of cell-death-associated genes with prognostic implications in bladder cancer. *Front Immunol*. 2022;13:909324. https://doi.org/10.3389/fimmu.2022.909324.
12. Li H, Lin Z, Zhuo J, et al. TNFR2 is a potent prognostic biomarker for post-transplant lung metastasis in patients with hepatocellular carcinoma. *Chin J Cancer Res*. 2023;35:66–80. https://doi.org/10.21147/j.issn.1000-9604.2023.01.07.
13. Zhuo JY, Lu D, Lin ZY, et al. CC motif chemokine ligand 16 inhibits the progression of liver cirrhosis via inactivating hepatic stellate cells. *Hepatobiliary Pancreat Dis Int*. 2020;19:440–448. https://doi.org/10.1016/j.hbpd.2019.12.006.
14. Bakir B, Chiarella AM, Pitarresi JR, Rustgi AK. EMT, MET, plasticity, and tumor metastasis. *Trends Cell Biol*. 2020;30:764–776. https://doi.org/10.1016/j.tcb.2020.07.003.
15. Zhou F, Elzi DJ, Jayabal P, et al. GDF6-CD99 signaling regulates Src and Ewing sarcoma growth. *Cell Rep*. 2020;33:108332. https://doi.org/10.1016/j.celrep.2020.108332.
16. Venkatesan AM, Vyas R, Gramann AK, et al. Ligand-activated BMP signaling inhibits cell differentiation and death to promote melanoma. *J Clin Invest*. 2018;128:294–308. https://doi.org/10.1172/JCI92513.
17. Chen H, Nio K, Tang H, et al. BMP9-ID1 signaling activates HIF-1α and VEGFA expression to promote tumor angiogenesis in hepatocellular carcinoma. *Int J Mol Sci*. 2022;23:1475. https://doi.org/10.3390/ijms23031475.
18. Cai C, Itzel T, Gaitantzi H, et al. Identification of liver-derived bone morphogenetic protein (BMP)-9 as a potential new candidate for treatment of colorectal cancer. *J Cell Mol Med*. 2022;26:343–353. https://doi.org/10.1111/jcmm.17084.
19. Chen H, Nio K, Yamashita T, et al. BMP9-ID1 signaling promotes EpCAM-positive cancer stem cell properties in hepatocellular carcinoma. *Mol Oncol*. 2021;15:2203–2218. https://doi.org/10.1002/1878-0261.12963.
20. Song K, Xu H, Wang C. The role of N6-methyladenosine methylation in the progression of endometrial cancer. *Cancer Biother Radiopharm*. 2022;37:737–749. https://doi.org/10.1089/cbr.2020.3912.
21. Wan P, Long E, Li Z, Zhu Y, Su W, Zhuo Y. TET-dependent GDF7 hypomethylation impairs aqueous humor outflow and serves as a potential therapeutic target in glaucoma. *Mol Ther*. 2021;29:1639–1657. https://doi.org/10.1016/j.ymthe.2020.12.030.
22. Sundqvist A, Morikawa M, Ren J, et al. JUNB governs a feed-forward network of TGFβ signaling that aggravates breast cancer invasion. *Nucleic Acids Res*. 2018;46:1180–1195. https://doi.org/10.1093/nar/gkx1190.
23. Wang L, Zhang X, Jia LT, et al. c-Myc-mediated epigenetic silencing of MicroRNA-101 contributes to dysregulation of multiple pathways in hepatocellular carcinoma. *Hepatology*. 2014;59:1850–1863. https://doi.org/10.1002/hep.26720.
24. Joung J, Kirchgatterer PC, Singh A, et al. CRISPR activation screen identifies BCL-2 proteins and B3GNT2 as drivers of cancer resistance to T cell-mediated cytotoxicity. *Nat Commun*. 2022;13:1606. https://doi.org/10.1038/s41467-022-29205-8.
25. Pérez-Benavente B, Fathinajafabadi A, de la Fuente L, et al. New roles for AP-1/JUNB in cell cycle control and tumorigenic cell invasion via regulation of cyclin E1 and TGF-β2. *Genome Biol*. 2022;23:252. https://doi.org/10.1186/s13059-022-02800-0.
26. Noguchi T, Ikeda M, Murakami M, et al. Regulatory expression of bone morphogenetic protein 6 by 2,2'-dipyridyl. *Biochim Biophys Acta Gen Subj*. 2020;1864:129610. https://doi.org/10.1016/j.bbagen.2020.129610.
27. Chen J, Song T, Yang S, et al. Snail mediates GDF-8-stimulated human extravillous trophoblast cell invasion by upregulating MMP2 expression. *Cell Commun Signal*. 2023;21:93. https://doi.org/10.1186/s12964-023-01107-2.
28. Liu B, Fu B, Zhou S, et al. Bone morphogenetic protein-9 downregulates StAR expression by inducing snail expression via SMAD1/5/8 signaling in human granulosa-lutein cells. *Mol Cell Endocrinol*. 2024;582:112126. https://doi.org/10.1016/j.mce.2023.112126.
29. Wu Z, Zhang Q, Wang H, et al. Growth differentiation factor-11 upregulates matrix metalloproteinase 2 expression by inducing Snail in human extravillous trophoblast cells. *Mol Cell Endocrinol*. 2024;585:112190. https://doi.org/10.1016/j.mce.2024.112190.
30. Roth P, Junker M, Tritschler I, et al. GDF-15 contributes to proliferation and immune escape of malignant gliomas. *Clin Cancer Res*. 2010;16:3851–3859. https://doi.org/10.1158/1078-0432.CCR-10-0705.